Tanzania Journal of Science 50(4): 898-911, 2024
ISSN 0856-1761, e-ISSN 2507-7961

Stellar Properties from a self-consistent Analysis

Pius Privatus[1,4*], Pulapa V Kanaka Rao[1] and Cirino Pappalardo[2,3]
[1]Department of Physics, The University of Dodoma, P.O.Box 338 Dodoma, Tanzania.
[2]Instituto de Astrof´ısica e Cie^ncias do Espac¸o, Universidade de Lisboa - OAL, Tapada da Ajuda, PT1349-018 Lisboa, Portugal
[3] Departamento de F´ısica, Faculdade de Cie^ncias da Universidade de Lisboa, Edif´ıcio C8, Campo Grande, PT1749-016 Lisboa, Portugal
[4]Department of Natural Sciences, Mbeya University of Science and Technology, Iyunga, Mbeya, 53119, Tanzania.
**Corresponding author. E-mail: privatuspius08@gmail.com, pvkrao76@gmail.com*
Received 8th Aug. 2024, Reviewed 30th Aug., Accepted 27th Oct., Published 30th Nov. 2024
https://dx.doi.org/10.4314/tjs.v50i4.15

Abstract

Galaxies' spectral energy distribution (SED) has been explored through the use of spectral synthesis codes. Most of the codes so far are solely stellar and assume a negligible nebular contribution. Fitting Analysis using Differential Evolution Optimisation (FADO) is the first spectral synthesis tool to consider the nebular contribution. The study examines how the primary stellar attributes are affected when FADO is applied to the Max Planck Institute for Astrophysics and Johns Hopkins University (MPA-JHU) data, namely the star-formation rate, metallicity, and stellar mass. The findings show that nebular emission results in the change of the slope of the equation of "the main sequence by 0.04 dex ", and " the vertical intercept by 0.3 dex ", and underestimates gas-phase metallicity of star-forming galaxies by 0.013.

Key Words: Nebular; spectral energy distribution; population spectral synthesis; SDSS.

Introduction

Fitting Analysis using Differential Evolution Optimization (FADO) is a Population spectral synthesis (PSS) approach that stands out for its ability to simultaneously identify the stellar as well as nebular components in a galaxy's spectrum in comparison to the solely stellar PSS tools (Cardoso et al. 2019). This particular, self-consistent code offers a novel method for analyzing the history of galaxies' assembly by minimizing the degeneracy typically present in conventional spectral synthesis techniques. It should be kept in mind that galaxies release electromagnetic radiation across the entire spectrum (Cardoso et al. 2022). Through analyzing this radiation, we can learn about its composition and physical characteristics. Spectral modeling is the study of a galaxy's spectrum across different wavelengths. Spectral modeling is a common technique used to determine the galaxies' physical characteristics. By examining a galaxy's spectrum synthesis techniques for panchromatic spectral energy distribution (SED), researchers can retrieve and interpret its physical properties. These methods have been instrumental in the finding of essential elements of current theories of galaxy evolution (Bamford et al. 2009, Conroy 2013, Kauffmann et al. 2003, Walcher et al. 2011). The different spectra of billions of stars and the nebular emissions brought on by their radiation make up the nuclear spectrum of a galaxy. Additionally, it contains thermal and non-thermal emissions coming from active galaxies, hot dust, and massive shocks in the multi-phase interstellar medium, among other things. These components combine to provide a thorough SED that illustrates the

mechanisms and development of a galaxy's energy generation and assembly across time (Kauffmann et al. 2004, Conroy 2013, Walcher et al. 2011).

PSS is a crucial instrument in extragalactic astronomy and aims to determine the fundamental morphological and evolutionary characteristics of galaxies over cosmic time (Panter et al. 2008). The objective of PSS is to use the galaxy's spectral energy distribution to determine its chemical enrichment history (CEH) and star formation history (SFH). The PSS technique is used to infer the mass, age, and metallicity of a galaxy's stellar populations from its spectrum. It is also known as the inverse, semi-empirical evolutionary, or fossil record technique. This approach works alongside evolutionary synthesis and has been effectively applied to vast spectroscopic datasets, notably the Sloan Digital Sky Survey (SDSS), resulting in valuable knowledge about the past and formation of galaxies (Panter et al. 2008). The galaxies' physical properties related to galaxies' formation and evolution are extracted from the spectra, such as star formation rates (SFRs), stellar masses, and gas phase metallicity (Brinchmann et al. 2004, Kauffmann et al. 2004). The primary limitation of current PSS techniques (for example STARLIGHT) is that they do not account for nebular emission (ne), leading to a lack of physical interpretation of the observed emission line (Gomes and Papaderos 2017). The deduced physical characteristics of a galaxy may therefore be biassed (Gomes and Papaderos 2017, Juneau et al. 2014). Furthermore, the method failed to distinguish between Pop III and Pop II star formation sites, in deed the biases present in codes that solely consider the stellar component (PS codes) can have significant astrophysical consequences. These include an amplified dispersion or alteration in the slope of the star formation main sequence (SFMS) and other scaling relationships, such as the relationship between stellar mass and metallicity.

The study conducted by Cardoso et al. (2022), compares the performance of FADO and STARLIGHT in estimating the galaxies' physical characteristics based on their spectral energy distributions. The authors compared the outcomes of the two techniques and the physical properties that were compared included stellar mass, and estimates of metallicity the results of the comparison showed that for galaxies where the nebular contribution is large, STARLIGHT tended to underestimate the stellar mass ($M_{\star}$) by 2 dex and mass-weighted mean stellar age by 4 dex. Furthermore, STARLIGHT tended to overestimate by up to 0.6 dex both the mean metallicity and light-weighted mean stellar age. On the other hand, FADO was found to provide significantly better estimates, even at stages of evolution where the nebular contribution was very significant, with a precision of 0.2 dex while the accuracy for STARLIGHT was only 0.1 dex on average. Overall, the research indicates that FADO is a more reliable method than STARLIGHT for determining the physical characteristics of galaxies from their spectra, especially when there are large nebular contributions.

Cardoso et al. (2022) used the Hα and Hβ flux measurements from the SDSS spectral database to estimate the nebular extinction and calculate the Hα luminosity, which was then used to estimate the SFR for a collection of low redshift star-forming galaxies. A comparison of data from the MPA-JHU catalog and FADO was created by using the estimated stellar mass and SFR from both techniques to obtain the SFMS for these galaxies. The stellar mass and SFR estimates from FADO and MPA-JHU were then combined to produce the SFMS. The study discovered that the deduced physical characteristics of star-forming galaxies in the local universe were not considerably impacted by the inclusion of the nebular continuum in FADO. Using Hα flux flow as a tracer, the SFR estimations from the MPA-JHU catalog and FADO were in good agreement. The differences obtained for stellar mass were negligible when considering the uncertainties. These results were attributed to the low nebular contribution in the majority of normal star-forming galaxies in the SDSS. However, the study notes that at higher redshifts, the expected increased nebular contribution might lead to different physical properties for

galaxies when using FADO (Miranda et al. 2023).

The primary goal of this work is to investigate how the major galactic characteristics of nearby galaxies evaluated in SDSS data release 8 are impacted by considering the nebular in the analysis. The structure of this paper is as follows: Material and Methods describes the survey used to collect the data, specifically the MPA-JHU, as well as the FADO analysis. Results present the findings of the study. The discussion shows the implications of the findings. Finally, the Conclusion shows a summary of the study.

Material and Methods

In this study, the galaxies under investigation were obtained from the sample of the SDSS, which is a wide-field optical survey that uses a 2.5 m f/5 modified Ritchey-Chretien telescope for conducting multi-spectral imaging and spectroscopic redshift measurements (York et al. 2000). The telescope is located at Apache Point Observatory in southeast New Mexico and sits at an altitude of 2,788 m. The SDSS collected data on objects that cover more than $14500\ \mathrm{deg}^2$ and extend to galaxies with a maximum magnitude of 23 in the g-band. This data release contains 1472581 objects with wavelength ranges $3800 - 9200$Å at a resolution of R ~ $1800 - 2200$ (Cardoso et al. 2017).

Stars, galaxies, or quasars are identified by their spectra in the SDSS. Redshifts are calculated automatically using two separate pipelines, the first is spectro1d, which uses cross-correlation with a family of templates and emission-line fits, and the second is the idlspec2d or specBS, which performs direct $\chi 2$ fitting of templates to the spectra (Aihara et al. 2011). Spectra are used to calculate emission line fluxes for galaxies. It is crucial to correctly consider the galaxy continuum, which is full of star absorption features while measuring the nebular emission lines of galaxies.

MPA-JHU

The MPA-JHU measurements provide various physical properties of galaxies, including star formation rates, stellar masses, and metallicities, derived from fitting the SDSS spectra with stellar population synthesis models (Brinchmann et al. 2004, Kauffmann et al. 2003). These measurements have been widely used in various studies of galaxy evolution, and the data set is considered reliable due to its photometric completeness, uniform spectral calibration, and wide redshift coverage (Aihara et al. 2011). To calculate star formation rates, Brinchmann et al. (2004) used the Hα emission line, which is a tracer of recent star formation activity. The SFR output corresponds to the probability distribution functions at the median, 2.5%, 16%, 84%, and 97.5% values. It is crucial to keep in mind that the star formation rates (SFRs) determined in this manner only reflect the star formation activity found inside the SDSS spectroscopic fibre aperture, which is a very limited area in comparison to the entire galaxy. Salim et al. (2015) use galaxy photometry SFRs outside of the fibre, and for AGN and galaxies with weak emission lines, SFRs are estimated from the SED. The report provides both the fibre SFR and the total SFR at different percentile levels of the distribution function. To estimate the nebular oxygen abundances, the authors use the Bayesian approach described in Tremonti et al. (2004) on the strong optical emission lines, including [OII]λ3727, Hα, Hβ, [OIII]λ5007, [NII]λ6548, 6584, and [SII]λ6717,6731. Only objects identified as star-forming are used to determine oxygen abundance. At the median and various percentile levels of the probability distribution function, the output value of 12+log(O/H) is provided. In summary, the paper presents an estimate of SFRs and nebular oxygen abundances for different types of galaxies using photometry and spectral information. The results are reported at different percentile levels of the probability distribution function, allowing for a better understanding of the uncertainties associated with the estimates.

FADO

FADO is a PSS tool capable of fitting the optical spectral energy distribution while considering the self-consistent contributions of both the stellar and nebular components. This innovative method of SED fitting is expected to have a significant effect on our

understanding of how the presence of nebular emission affects our interpretation of spectroscopic data and our understanding of the physical processes occurring within galaxies (Miranda et al. 2023; Pappalardo et al. 2021). To assess the capabilities of FADO, a series of benchmark publications have been carried out, including Cardoso et al. (2019), Pappalardo et al. (2021), and Miranda et al. (2022). These studies demonstrate the accuracy and reliability of FADO in reproducing observed SEDs and in recovering key physical properties of galaxies.

Overall, FADO represents a considerable advancement in population spectral synthesis and is well-positioned to significantly advance our knowledge of the intricate interactions between stars and gas in galaxies. The population synthesis codes were applied to the SDSS DR8. According to Gomes and Papaderos (2017), the population synthesis algorithm FADO's primary function is to linearly combine spectral components that are typical of individual star spectral (SSPs) to reproduce the observed SED as expressed by Equation 1.

$$F_\lambda = \sum_{i=1}^{N_\star} M_{i,\lambda_0} \times L_{i,\lambda} \times 10^{-0.4\times A_v \times q_\lambda} \otimes S(\nu_\star, \sigma_\star) + \Gamma_\lambda(n_e, T_e) \times 10^{-0.4\times {A_v}^{neb} \times q_\lambda} \otimes N(\nu_\eta, \sigma_\eta) \ldots\ldots\ldots\ldots\ldots 1$$

where: F_λ is the flux observed from the spectrum; $N_\star$ is the number of distinct spectral components in the adopted base library; M_{i,λ_0} is the stellar mass of the spectral component i at the normalization wavelength, $L_{i,\lambda}$ is the luminosity contribution of the i^{th} spectral component; A_v is the V-band extinction; q_λ is the ratio of A_λ over A_v; $S(\nu_\star, \sigma_\star)$ denotes a Gaussian kernel simulating the effect of stellar kinematics on the spectrum, with $\nu_\star$ and $\nu_\star$ $\sigma_\star$ representing the stellar shift and dispersion velocities, respectively; $\Gamma_\lambda(n_e, T_e)$ is the nebular continuum computed assuming that all stellar photons with $\lambda \leq 911.76$Å are absorbed and reprocessed into nebular emission, under the assumption of case B recombination, this arises when the ionizing photons are of lower energy ($E \leq 13.6$ eV). Case A recombination is when the ionizing photon has higher energy ($E \geq 13.6$ eV). ${A_v}^{neb}$ is the nebular V-band extinction, and $N(\nu_\eta, \sigma_\eta)$ denotes the nebular kinematics kernel, with ν_η and σ_η representing the nebular shift dispersion, respectively. It is important to note that before the creation of FADO, population synthesis codes that were made available to the general public were created using only the first term of Equation 1. This indicates that the whole observable spectral energy distribution (SED) of galaxies was created using only a purely stellar approach (Cardoso et al. 2022).

FADO's inclusion of the second term in Equation 1, which accounts for the contribution of the nebular continuum component, is a unique and important feature that sets it apart from previous population synthesis codes. This feature enables FADO to more accurately model the observed SEDs of the galaxies and to better constrain their physical properties.

For example, the presence of nebular emission can lead to an overestimation of the $M_\star$ and an underestimate of the SFR if not properly accounted for. FADO's ability to self-consistently model both components is, therefore, an important advance in the field of population synthesis, and has the potential to increase our knowledge of the physical mechanisms governing galaxy evolution.

Selection criteria

The signal-to-noise ratio (S/N) is commonly used in spectroscopic studies to ensure the quality of the data and to minimize the effects of random errors. This ensures that the measured line fluxes are reliable and that the emission lines are not dominated by noise. In this study, the S/N cut 3 for NII, SII, OI, Hβ, and Hα was applied to be consistent with other studies for easy comparison of the results (Kewley et al. 2006, Veilleux and Osterbrock 1987).

The theoretical value flux ratios $F\left(\frac{H\alpha}{H\beta}\right)$ are derived from the physics of the hydrogen atom and the Balmer series of spectral lines. In the

case of optically thick nebulae, where the photons emitted after recombination are absorbed locally, the ratio of the hydrogen Balmer lines Hα and Hβ can be used to determine the extinction due to dust in the nebula. Assuming that the electron temperature is $T = 10^4$ K and the electron density, $ne \sim 10^2 - 10^4\ cm^{-3}$, the theoretical value flux ratios $F\left(\frac{H\alpha}{H\beta}\right)$ are 2.86 and 3.1 for star-forming and AGNs, respectively (Kewley et al. 2001, 2013). These values serve as a reference to compare with the observed Balmer decrement, which is the ratio of the observed Hα and Hβ fluxes and can be used to estimate the amount of dust extinction in the nebula. It is common practice to remove objects with Balmer decrements that are lower than the theoretical values for their respective classifications. This is done to avoid misclassifying objects as AGNs when they are star-forming galaxies with a low Balmer decrement due to factors such as low reddening, inaccuracies in the stellar absorption correction, or errors in the measurement of line flux. In this study, objects with $F\left(\frac{H\alpha}{H\beta}\right) < 2.86$ for star-forming galaxies and with $F\left(\frac{H\alpha}{H\beta}\right) < 3.1$ for AGNs were removed from the sample to ensure accurate classification. The median redshift of the objects used in this study is at $z \sim 0.1$.

Results

The galaxies classification

The galaxies were classified based on the methods of Kewley et al. (2006) as shown in Table 1. The total sample of star-forming, composite, Seyfert, and LINER galaxies by cross-correlation. Star-forming galaxy numbers were obtained by cross-matching star-forming galaxies for NII BPT and star-forming + composite galaxies for both SII and OI diagrams as shown in Figure 1 and Table 2. Cross-matching the number of SF for both MPA-JHU and FADO the total number of 127283 Star-forming galaxies was obtained. Composite galaxy numbers were obtained by cross-matching Composite galaxies for NII-BPT, with Star-forming and Composite for both SII and OI classification diagrams as shown in Figure 2 and Table 3. Cross-matching the number of Composite galaxies for both MPA-JHU and FADO the total number of 13337 Composite galaxies was obtained. Seyfert 2 galaxy numbers were obtained by cross-matching Seyfert 2 galaxies for NII BPT, SII, and OI classification diagrams as shown in Table 4. Cross Matching the number of Seyfert2 galaxies for both MPA-JHU and FADO the total number of 8391 Seyfert2 galaxies were obtained. LINER galaxies were obtained by cross-matching Liner galaxies for NII BPT, SII, and OI classification diagrams as shown in Table 5. Cross-matching the number of LINER galaxies for both MPA-JHU and FADO the total number of 3447 LINER galaxies was obtained.

Properties of emission lines

Since the SFR was derived from Hα flux and the ratio of the hydrogen Balmer lines Hα and Hβ was used to determine the extinction due to dust in the nebula. The features of the emission lines that MPA-JHU and FADO have retrieved must be described. It is important to understand the connection between the observed flux of an emission line that is typical for FADO and MPA-JHU as will be used to trace the SFR hence the stellar mass against SFR relation.

Table 1: The Total number of galaxies for the diagnostic diagrams

Galaxies Cross matched	**MPA-JHU & FADO**			
	Star Forming	Composite	Seyfert	LNERs
NII vs SII	220919	49153	11391	7311
NII vs OI	129389	13503	9388	3986
SII vs OI	145762	145762	9430	6286
(NII vs SII) vs (SII vs OI)	127283	13337	8391	3447

The sample of 127283 Star-forming,13337 composite, 8391 Seyfert, and 3447 LINERs galaxies are used in the next sections unless otherwise stated.

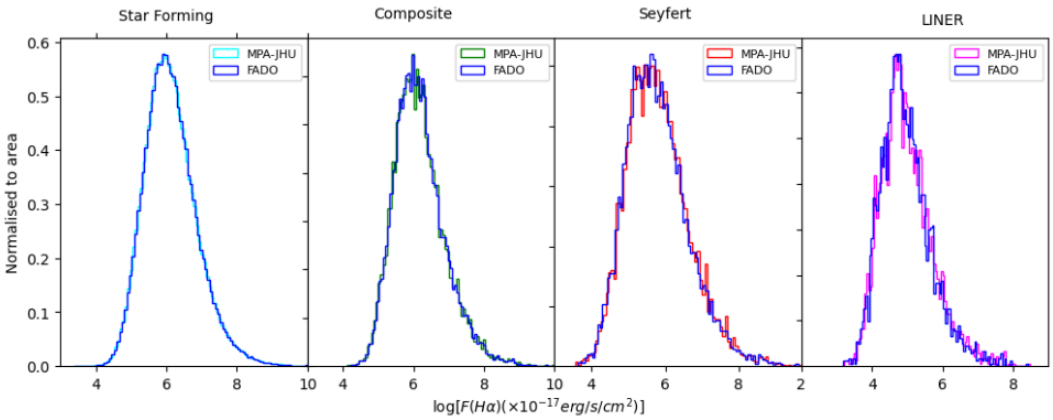

Figure 1: Comparisons of Hα flux between MPA and FADO

Table 2: The median differences for the Hα flux between FADO and MPA-JHU.

Median Hα Flux (erg/s/cm^2)			
Galaxy type	MPA-JHU	FADO	FADO−MPA-JHU
Star-forming	6.048	6.050	0.002
Composite	6.084	6.088	0.004
Seyfert	5.690	5.72	0.030
LINERs	4.849	4.884	0.035

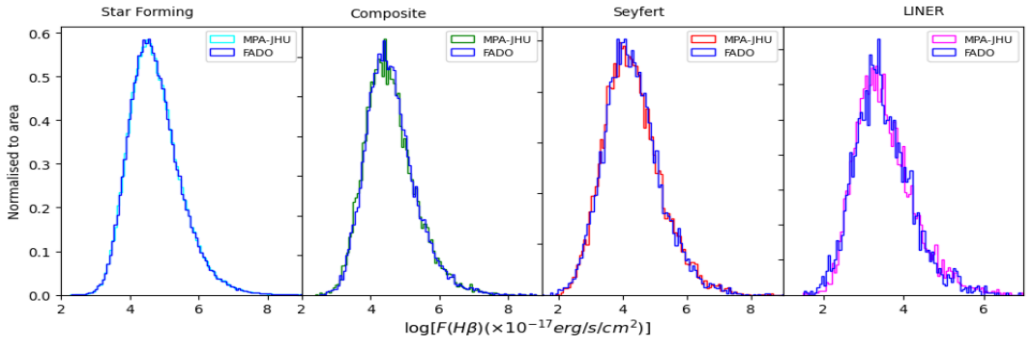

Figure 2: Comparisons of Hβ flux between FADO and MPA-JHU

Table 3: The median difference for Hβ Flux between FADO and MPA-JHU

Median Hβ Flux (erg/s/cm^2)			
Galaxy type	MPA-JHU	FADO	FADO−MPA-JHU
Star-forming	4.638	4.642	0.004
Composite	4.480	4.500	0.020
Seyfert	4.209	4.210	0.001
LINERs	3.400	3.420	0.020

Star formation rate

The flux was used as the tracer for the Star formation rate using Equation 2 and the Luminosity using Equation 3.

$$SFR_f = \frac{L(H\alpha)}{\eta(H\alpha)} \ldots\ldots\ldots\ldots\ldots\ldots\ldots\ldots\ldots\ldots\ldots\ldots 2$$

where, L(Hα) is the Hα luminosity and η(Hα) is a conversion factor. The conversion factor η (Hα) depends on the initial mass function (IMF), which explains how the star masses are distributed in a specific population.

Remembering that different IMFs can result in different η (Hα) values, due to the factor that the number of ionizing photons produced by stars of different masses varies thus the choice of IMF can affect the estimated SFR by a factor of a few. The commonly used IMFs include the Salpeter IMF and the Chabrier IMF at which the Salpeter IMF generally results in higher SFR estimates than the Chabrier IMF.

Other factors that can affect the estimation of SFRs include the presence of dust, which can absorb and re-emit ionizing radiation, furthermore the calibration of the η(Hα) factor itself also may affect the SFRs estimation, which varies depending on assumptions made about the stellar population.

In this study, we used the Kennicutt . (1998) conversion factor as the best estimator given by:$\eta(H\alpha) = 10^{41.28} ergs^{-1} M_{\odot}^{-1} yr$ (Kauffmann et al. 2004).

$$L(H\alpha) = F(H\alpha) \cdot 4\pi d^2 \ldots\ldots\ldots\ldots\ldots\ldots\ldots 3$$

where, F(Hα) is the Hα flux and (d) is the luminosity distance.

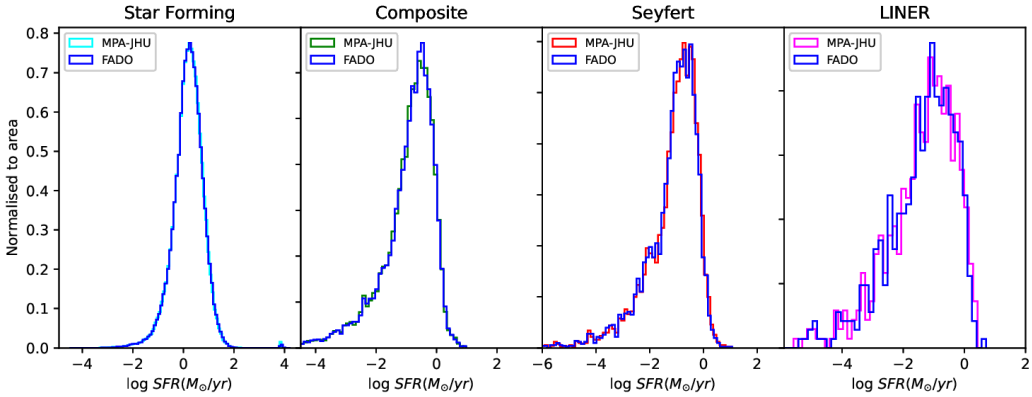

Figure 3: Comparison of Total SFR for MPA-JHU and FADO.

From Figure 3 it is shown that both FADO and MPA- JHU have similar distribution for total SFR indicating that the interior physical properties underlying the star formation activities are similar.

Table 4: The difference between the median values of FADO distribution to MPA-JHU for Total SFR

	Median Total SFR ($M_\odot$/yr)		
Galaxy type	MPA-JHU	FADO	FADO-MPA-JHU
Star-forming	-1.521	-1.520	0.001
Composite	-1.019	-1.018	0.001
Seyfert	-3.200	-3.170	0.030

LINERs	-0.110	-0.160	0.050

From Table 4 it is observed that FADO overestimates the SFR over MPA-JHU for all classes of galaxies. The account for this is the method used for obtaining fluxes that is for FADO to consider, the nebular continuum as shown by Equation 1 above whereas MPA-JHU does not that is consider only the first part of Equation 1. This fact has a slightly significant impact on the measured flux of emission lines, such as Hα, hence on the estimation of SFR since the nebular continuum assumed by FADO is the main foundation of galaxy formation and evolution, considering this important part results to the rise of SFR the results obtained by FADO are more reliable.

The Stellar Mass

The star masses found in the MPA-JHU library adhere to a similar mindset to that of Kauffmann et al. (2003). In Kauffmann et al. (2003), the SED was fitted using several models from Charlot and Fall (2000), and spectroscopic features were considered using five observation windows used by SDSS surveys are the u, g, r, i, and z photometry. The stellar mass is calculated from these fits by estimating the stellar mass-to-light ratio but for the case of FADO, the stellar mass was obtained by fitting the SED.

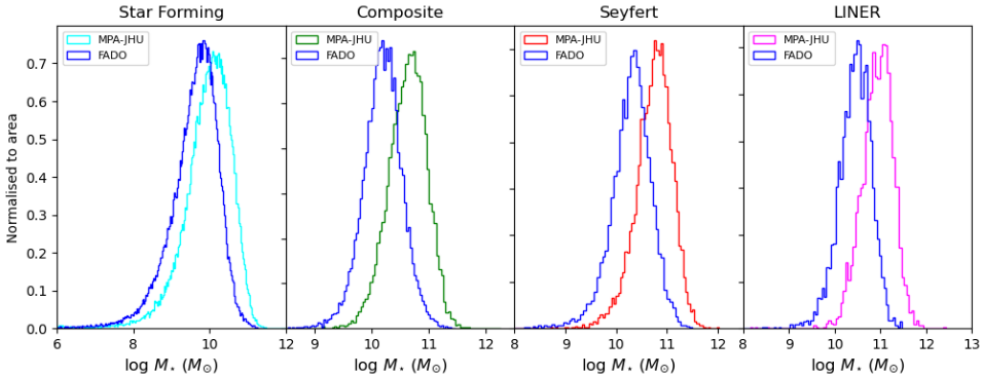

Figure 4: The total stellar mass Histogram plots for MPA-JHU and FADO.

Table 5: The median Total Stellar Mass between FADO and MPA-JHU

Median Total Stellar Masses ($M_\odot$)			
Galaxy type	MPA-JHU	FADO	FADO-MPA-JHU
Star-forming	10.01	9.67	-0.34
Composite	10.64	10.18	-0.45
Seyfert	10.76	10.31	-0.45
LINERs	10.54	10.46	-0.48

From Figure 4 it is shown that FADO underestimates the Stellar mass over MPA-JHU and Table 5 it is shown that FADO underestimates the Stellar mass over MPA-JHU on average by 0.43 dex. This is due to FADO considering the nebular continuum, variations in results for star mass between FADO and MPA-JHU data were achieved. Using the stellar continuum, the stellar mass is approximated. The observed continuum is thought to be entirely the result of star emission when using pure stellar coding, as is the case for the MPA-JHU catalog data. FADO, on the other hand, detects a continuum with both stellar and nebular components. In comparison to the stellar continuum used to estimate the MPA-JHU catalog data, this has the effect of decreasing the stellar continuum

for FADO. Because of this, FADO obtains lower stellar masses than those from MPA-JHU when the stellar continuum is used to estimate stellar mass. This is different from the case obtained in Table 4 where the SFR is approximated by both stellar continuum and nebular continuum making the SFR for FADO to be higher than MPA-JHU Both the results support the observations from galaxies models predicting the increase of SFR and decrease of stellar mass when the nebular continuum is considered.

Metallicity

The methods discussed in the Methodology section were used as the gas phase metallicity estimator. For Figure 5, Left panel: Histogram for FADO (blue) and MPA-JHU (magenta). Middle and right panel: 1-1 scatter and contour plot, respectively. The median for the MPA-JHU metallicity was found to be 8.947 and 8.934 for FADO. The median difference in metallicity between MPA-JHU and FADO is 0.013 dex (3%).

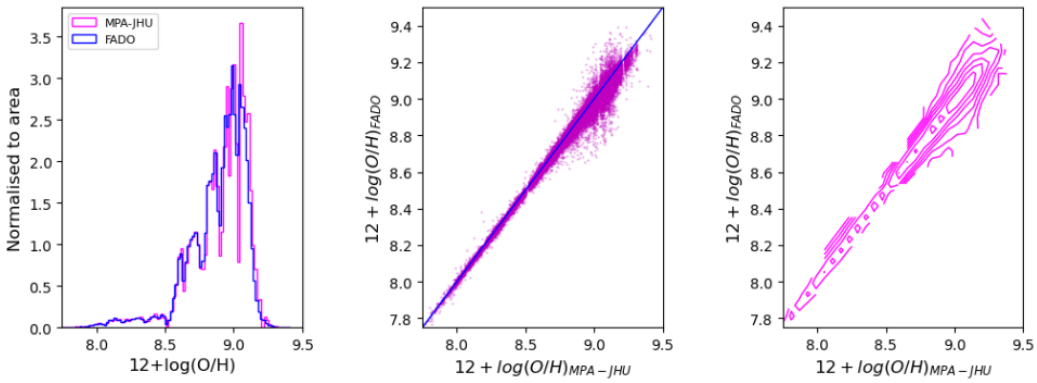

Figure 5: Gas phase metallicity histogram plots for MPA-JHU and FADO.

The Main Sequence

In this subsection, the Star-formation rate Versus Stellar mass relation of the Star-forming, Composite, Seyfert, and LINER galaxies classified sample for both MPA-JHU and FADO was discussed. We generate the equation of the main sequence and show the position of the galaxies. Upper panels: Scatter plot, Bottom panel: Contour plot showing the distribution of sources in the diagram. The contour plots show the sample's 20%, 40%, 60%, 80% and 100%. It was obtained that FADO overestimated the SFR and underestimated the Stellar mass relative to MPA-JHU. This subsection aims to study the main sequence by combining these galactic properties (the SFR and Stellar mass). The general equation of the best-fit line was adopted from Leslie et al. (2015), for our data is given by Equation 4 for MPA-JHU and Equation 5 for FADO.

$$\log(\mathrm{SFR}) = 0.77\log(\mathrm{M}\star) - 7.5 \quad \ldots\ldots\ldots 4$$

$$\log(\mathrm{SFR}) = 0.73\log(\mathrm{M}\star) - 7.2 \quad \ldots\ldots\ldots 5$$

For the width of the main sequence $\pm(0.3)$ dex (dashed lines) was used (Elbaz et al., 2007; Whitaker et al., 2012; Shimizu et al., 2015) The location of every galaxy in our sample for the main sequence is shown in Table 6 and the star formation rate versus stellar mass diagram is shown in Figure 6. From Figure 6, the application of FADO causes the y-intercept and slope of the main sequence equation to alter by 0.3 and 0.04 dex, respectively.

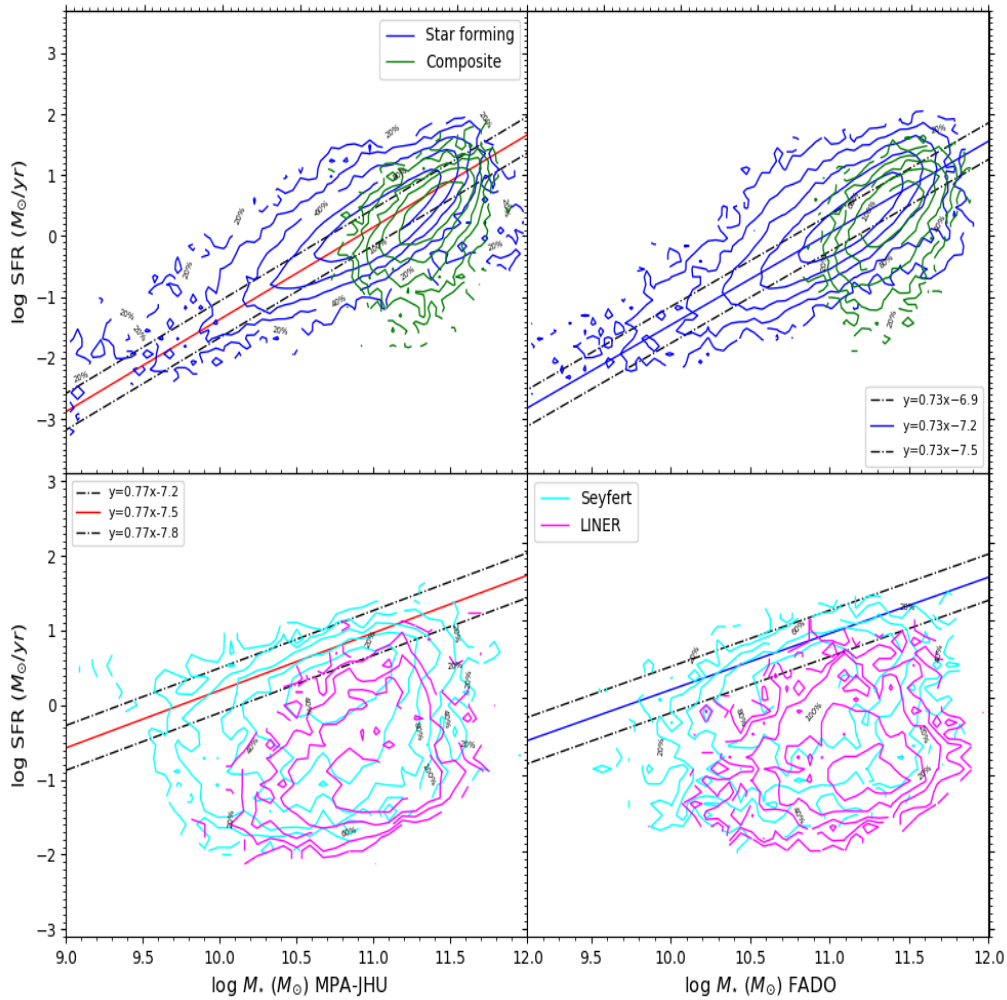

Figure 6: Position of galaxies concerning the Main sequence for MPA (left panels) and FADO (right panels)

Table 6: The number of galaxies above, below, and within the main sequence

	Number of Galaxies							
	Star-forming		Composite		Seyfert		LINERs	
Position	MPA	FADO	MPA	FADO	MPA	FADO	MPA	FADO
Above MS	24265 (19%)	20923 (16%)	393 (3%)	574 (4%)	86 (1%)	154 (2%)	5 (0%)	8 (0%)
Below MS	18726 (15%)	27496 (22%)	7779 (58%)	6874 (52%)	6755 (81%)	6425 (77%)	3375 (98%)	3346 (97%)
Within MS	84292 (66%)	78708 (62%)	5165 (39%)	5875 (44%)	1550 (18%)	1775 (21%)	67 (2%)	90 (3%)

From Table 6 it was observed that for Star-forming galaxies a greater number of galaxies (4%) are within the main sequence for pure stellar codes (MPA) when compared to non-pure stellar code (FADO). For composite galaxies, a smaller number of galaxies (5%) are within the main sequence for MPA when compared to FADO. For Seyfert galaxies, a smaller number of galaxies (3%) are within the main sequence MPA when compared to FADO. For composite galaxies, a smaller number of galaxies (1%) are within the main sequence for MPA when compared to FADO. This implies that the inclusion of nebular alters the star formation's main sequence.

Mass-Metallicity Relation

From Figure 4 and Table 5, it was obtained that FADO overestimated the Stellar mass and from Figure 5, FADO underestimated the gas phase metallicity relative to MPA-JHU. The gas phase metallicity Versus Stellar mass relation of the Star-forming galaxies classified sample was discussed, for both MPA-JHU and FADO as shown in Figure 7, the line of best fit (red and blue dashed lines, respectively) (adopted from Tremonti et al. (2004)) given by Equation 6 for MPA-JHU and Equation 7 for FADO. Top panel: Scatter plot. Bottom panel: The contour plots show the sample's 20%, 40%, 60%, 80% and 100%. From Figure 7, the distribution of gas phase metallicity is similar for both MPA-JHU and FADO although there is a shift in the equation of the best fit.

Discussion

Over earlier spectral synthesis techniques, FADO has a major astrophysical advantage in estimating physical parameters in the MPA-JHU catalog. The spectral energy distribution fitting procedure used by FADO incorporates the nebular component, resulting in an overall continuum that combines the stellar and nebular continuums. In contrast, earlier techniques assumed that the stellar contribution to the continuum as a whole was purely stellar and only took it into account.

The primary innovation of FADO from an astrophysical standpoint, as studied by Cardoso et al. (2022) and Miranda et al. (2022), is the addition of the nebular component in the SED fitting procedure. The purpose of the study was to compare the physical parameters obtained from fitting the SED with FADO versus utilizing conventional stellar models. The findings demonstrated that the nebular component's inclusion enhanced the measured spectra's fit and produced more precise calculations of the physical characteristics, including metallicity and star formation rate. It is useful to contrast and evaluate our results in light of past studies' conclusions because they have looked into themes that are connected to the one we are studying.

Cardoso et al. (2022) explored how the incorporation of the nebular input in the fitting process of the SED affects the evolutionary trend of light- and mass-weighted parameters linked to the star age, metallicity, and mass of SF galaxies. They examined various subsets of galaxies based on their star production level, which was measured by the equivalent width of their emission lines, and contrasted this method to earlier ones, including the one used in MPA-JHU. They also examined several subsamples based on the Equivalent width as a measure of the star formation level. The goal was to understand how the nebular continuum contribution changed the star properties of the galaxies in the different subsamples. One of the main findings of this study was that, even though FADO yielded stellar masses that were higher than those of STARLIGHT, the estimated stellar mass changes when the nebular continuum is considered.

Miranda et al. (2022), found that for normal star-forming galaxies in SDSS, including the nebular contribution in the modeling process does not significantly impact the retrieved Hα fluxes and therefore does not affect the resulting SFR estimations based on the extinction corrected Hα luminosity. Additionally, they discovered that the stellar mass estimations between MPA-JHU catalog data and FADO are comparable, demonstrating that the inclusion of the nebular component has no impact on the stellar mass estimates in both galaxies.

However, the agreement between the two methods may not hold for higher redshift galaxies, as the expected increased nebular

contribution could lead to different physical properties. Using FADO we managed to prove the importance of nebular continuum to the derived properties of the galaxies for star-forming, Composite, Seyfert, and LINERs and trace the impact of nebular continuum on stellar mass and SFR relations.

Conclusion

The unique spectral synthesis code, FADO, was studied in this work. By applying FADO to the Sloan Digital Sky Survey and analyzing the major characteristics of the galaxies such as stellar mass, SFR, and gas phase metallicity. The peculiarity of FADO, which considers both stellar and nebular components when fitting a galaxy's spectrum, was investigated. The typical galaxies between the MPA-JHU and FADO were found by cross-correlation using the S/N>3 condition.

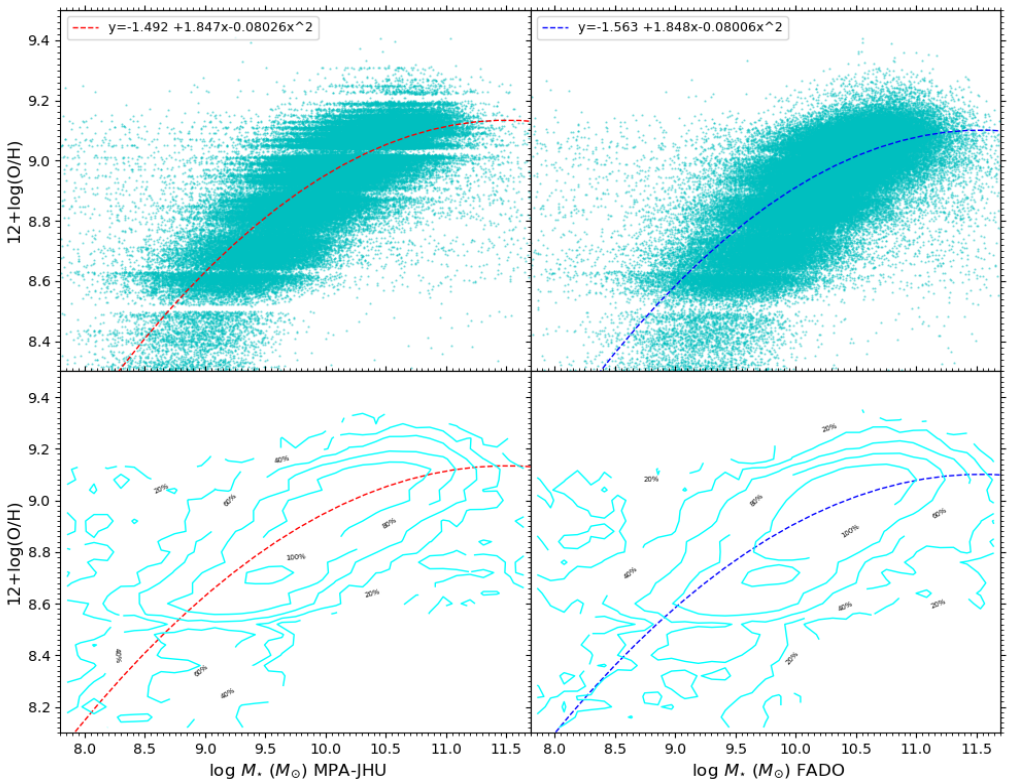

Figure 7: The Stellar mass against gas phase metallicity relation for MPA -JHU and FADO

$$12+\left(\frac{O}{H}\right)=-1.492+1.847\log(M\star)-0.08026\log(M\star)^2 \quad \ldots\ldots 6$$

$$12+\left(\frac{O}{H}\right)=-1.563+1.848\log(M\star)-0.08006\log(M\star)^2 \quad \ldots\ldots 7$$

The galaxies were classified into Star-forming, Composite, Seyfert, and LINER using the appropriate conditions (Kewley et al. 2001, Tremonti et al. 2004). The Balmer decrement conditions were applied to the classified samples for both MPA- JHU and FADO. The galaxies properties (Star formation, stellar mass, and gas phase metallicity) of the total number of galaxies

under each classification were discussed, and the important findings of this study are:

- Taking the nebular continuum into account improves the fluxes of star-forming, Composite, Seyfert, and LINER galaxies.
- FADO overestimates the star formation rate and underestimates the stellar mass of star-forming, Composite, Seyfert, and LINER galaxies.
- FADO underestimates gas-phase metallicity of star-forming galaxies over MPA-JHU by 0.013 dex (3%).
- Applying FADO to the MPA-JHU results in the change of the slope of the equation of the main sequence by 0.04 dex and the vertical intercept by 0.3 dex.

- FADO results in the modification of the best fit equation, in the stellar mass metallicity relation.

Acknowledgments

We acknowledge the Max Planck Institute for Astrophysics and Johns Hopkins University for providing the data necessary for this study. C.P. acknowledges support from DL57/2016 (P2460) from the 'Departamento de F´ısica, Faculdade de Cieˆncias da Universidade de Lisboa'.

References

Aihara H, Allende Prieto C, An D … Shu Y 2011 The eighth data release of the sloan digital sky survey: First data from SDSS-III. *Astrophys. J. Suppl. Ser.* 193(2): 29 https://doi.org/10.1088/0067-0049/193/2/29

Bamford SP, Nichol RC, Baldry IK, Land K, Lintott CJ, Schawinski 2009 Galaxy Zoo: The dependence of morphology and colour on the environment. *Mon. Not. R. Astron. Soc.* 393(4): 1324–1352. https://doi.org/10.1111/j.1365-2966.2008.14252.x

Brinchmann, J., Charlot, S., White, S. D. M., Tremonti C, Kauffmann G, 2004 The physical properties of star-forming galaxies in the low-redshift Universe. *Mon. Not. R. Astron. Soc.* 351(4): 1151–1179. https://doi.org/10.1111/j.1365-2966.2004.07881.x

Cardoso LS, Gomes JM, & Papaderos P 2017 Impact of an AGN featureless continuum on estimation of stellar population properties. *Astron. Astrophys*. 604: A99. https://doi.org/10.1051/0004-6361/201630378

Cardoso LSM, Gomes JM, &Papaderos P 2019 Self-consistent population spectral synthesis with FADO: I. the importance of nebular emission in modelling star-forming galaxies. *Astron. Astrophys*. 622: 1–24. https://doi.org/10.1051/0004-6361/201833438

Cardoso LS, Gomes JM, Papaderos P, Pappalardo C, Miranda H, Paulino-Afonso A, & Lagos P 2022 Revisiting stellar properties of star-forming galaxies with stellar and nebular spectral modelling. *Astron. Astrophys*. 667: A11. https://doi.org/10.1051/0004-6361/202243856

Charlot S, & Fall SM 2000 A simple model for the absorption of starlight by dust in galaxies. *Astrophys. J.* 539(2): 718. https://doi.org/10.1086/309250

Conroy C 2013 Modeling the panchromatic spectral energy distributions of galaxies. *Ann. Rev. Astron. Astrophys.* 51*:* 393–455. https://doi.org/10.1146/annurev-astro-082812-141017

Elbaz D, Daddi E, Le Borgne D, Dickinson M, Alexander DM, Chary RR, ... & Vanzella E. (2007). The reversal of the star formation-density relation in the distant universe. *Astron. Astrophys*. 468(1): 33-48. https://doi.org/10.1051/0004-6361:20077525

Gomes JM, & Papaderos P 2017 Fitting Analysis using Differential evolution Optimization (FADO): Spectral population synthesis through genetic optimization under self-consistency boundary conditions. *Astron. Astrophys.* 603. https://doi.org/10.1051/0004-6361/201628986

Juneau S, Bournaud F, Charlot S, Daddi E, Elbaz D 2014 Active galactic nuclei emission line diagnostics and the mass-metallicity relation: The impact of selection effects and evolution. *Astrophys. J.* 788(1): https://doi.org/10.1088/0004-637X/788/1/88

Kauffmann G, Heckman TM, Tremonti C,

Brinchmann 2003 The host galaxies of active galactic nuclei. *Mon. Not. R. Astron. Soc.* 346(4): 1055–1077. https://doi.org/10.1111/j.1365-2966.2003.07154.x

Kauffmann G, White SDM, Heckman TM, Ménard B 2004 The environmental dependence of the relations between stellar mass, structure, star formation and nuclear activity in galaxies. *Mon. Not. R. Astron. Soc.* 353(3): 713–731. https://doi.org/10.1111/j.1365-2966.2004.08117.x

Kennicutt Jr RC 1998 The global Schmidt law in star-forming galaxies. Astrophys. J. 498(2): 541. https://doi.org/10.1086/305588

Kewley, L. J., Dopita, M. A., Sutherland. (2001). Theoretical Modeling of Starburst Galaxies. *Astrophys. J.* 556(1): 121–140. https://doi.org/10.1086/321545

Kewley, L. J., Groves, B., Kauffmann, G., & Heckman, T. (2006). The host galaxies and classification of active galactic nuclei. *Mon. Not. R. Astron. Soc.* 372(3): 961-976. https://doi.org/10.1111/j.1365-2966.2006.10859.x

Kewley LJ, Maier C, Yabe 2013 THE cosmic BPT diagram: Confronting theory with observations. *Astrophys. J. Lett.* 774(1): 6–11. https://doi.org/10.1088/2041-8205/774/1/L10

Leslie, S. K., Kewley, L. J., Sanders, D. B., & Lee, N. (2015). Quenching star formation: insights from the local main sequence. *Mon. Not. R. Astron. Soc.* 455(1): L82-L86. https://doi.org/10.1093/mnrasl/slv135

Miranda, H., Pappalardo, C., Papaderos, P., Afonso, J., Matute, I., Lobo, C., Paulino-Afonso, A., Carvajal, R., Lorenzoni, S., &Santos, D. (2023). An investigation of the star-forming main sequence considering the nebular continuum emission at low-z. *Astron. Astrophys.* https://doi.org/10.1051/0004 -6361/202244390

Panter B, Jimenez R, Heavens AF & Charlot S 2008 The cosmic evolution of metallicity from the SDSS fossil record. *Mon. Not. R. Astron. Soc.* 391(3): 1117–1126. https://doi.org/10.1111/j.1365-2966.2008.13981.x

Pappalardo C, Cardoso LS, Gomes JM, Papaderos P, Afonso J, Breda I, ... & Miranda H 2021 Self-consistent population spectral synthesis with FADO-II. Star formation history of galaxies in spectral synthesis methods. Astron. Astrophys. 651: A99. https://doi.org/10.1051/0004-6361/202039792

Salim S, Lee JC, Davé R & Dickinson M 2015 On the Mass–metallicity–star formation rate relation for galaxies at z∼ 2. *Astrophys. J.* 808(1): 25. https://doi.org/10.1088/0004-637X/808/1/25

Shimizu TT, Mushotzky RF, Meléndez M, Koss M, & Rosario DJ 2015 Decreased specific star formation rates in AGN host galaxies. *Mon. Not. R. Astron. Soc.* 452(2): 1841-1860. https://doi.org/10.1093/mnras/stv1407

Tremonti CA, Heckman TM, Kauffmann G, Brinchmann 2004 The Origin of the Mass-Metallicity Relation: Insights from 53,000 Star-forming Galaxies in the Sloan Digital Sky Survey. *Astrophys. J.* 613(2): 898–913. https://doi.org/10.1086/423264

Veilleux S, & Osterbrock DE 1987 Spectral classification of emission-line galaxies. *Astrophys. J. Suppl. Ser.* 63: 295–310. https://ntrs.nasa.gov/api/citations/19870014941/downloads/19870014941.pdf

Walcher J, Groves B, Budavári T, & Dale D 2011 Fitting the integrated spectral energy distributions of galaxies. *Astrophys. Space Sci.* 331(1): 1–51. https://doi.org/10.1007/s10509-010-0458-z

Whitaker KE, Van Dokkum PG, Brammer G, & Franx M 2012 The star formation mass sequence out to z= 2.5. *Astrophys. J. Lett.* 754(2): L29. https://doi.org/10.1088/2041-8205/754/2/L29

York DG, Adelman J, Anderson Jr, JE, Anderson SF, Annis 2000 The sloan digital sky survey: Technical summary. *Astron. J.* 120(3): 1579. https://doi.org/10.1086/301513